Received: 13 February 2020 | Revised: 14 April 2020 | Accepted: 11 May 2020 | Published online: 25 June 2020

DOI: 10.1002/trc2.12040

Alzheimer's & Dementia
Translational Research & Clinical Interventions

RESEARCH ARTICLE

COSMC mutations reduce T-synthase activity in advanced Alzheimer's disease

Seema Gollamudi | **Rukmani Lekhraj** | **Shirin Lalezari** | **Parviz Lalezari**

Neurosurgery Research Laboratory, Department of Neurosurgery, Montefiore Medical Center and Albert Einstein College of Medicine, Bronx, New York, USA

Correspondence
Parviz Lalezari, Montefiore Medical Center, 111 East 210 Street, Neurosurgery Research Laboratory, Moses Research Tower, 3rd Floor, Bronx, NY 10467, USA.
Email: lalezari2@aol.com

Abstract

Introduction: Mutations in brain tissues that cumulate with age may contribute to Alzheimer's disease (AD). Abnormal glycoprotein and Tn antigen expression have been demonstrated in AD. We identified *C1GALT1C1/COSMC* mutations in AD and age-matched normals without AD. The *COSMC* coding mutations resulted in a significant reduction in T-synthase activity in advanced AD cases.

Methods: Identification of *COSMC* mutations, Real-Time Quantitative Reverse Transcription PCR (Q-RT-PCR), western blotting, and T-synthase activity assays.

Results: *COSMC* mutations were detected in the promotor, coding region and 3′UTR in AD and normals. *COSMC* coding mutations demonstrated a correlation with AD progression. T-synthase levels were significantly elevated in advanced AD compared to AD III ($P = 0.03$) and normals ($P = 0.002$). T-synthase activity in advanced AD {Braak and Braak (B&B) stages V and VI} with *COSMC* coding mutations was 3-fold lower than advanced AD without mutations, and 1.3-fold lower than normal ($P = 0.001$) and AD B&B stage III ($P = 0.01$) with coding mutations.

Discussion: *COSMC* coding mutations significantly diminished T-synthase activity in advanced AD, potentially causing defective galactosylation.

KEYWORDS
brain, C1GALT1/T-synthase, COSMC/C1GALT1C1, late-onset Alzheimer's disease, mutations

1 | INTRODUCTION

Since the discovery of Alzheimer's disease (AD) there have been many explorations to determine its pathogenesis. AD is classified as early onset (EOAD, ≤65 years) and late-onset (LOAD, >65 years).[1] In EOAD, which affects 5% of AD population, three autosomal dominant genes—amyloid precursor protein (APP), presenilin 1, and presenilin 2—are involved in the pathogenesis.[2] Genetic factors are considered to play a role in the pathogenesis of LOAD, but since their mechanisms of action are unknown, they are considered risk factors. These include polymorphisms in apolipoprotein E gene ε4 alleles, methylenetetrahydrofolate reductase, and brain-derived neurotrophic factor.[3,4] AD in different forms has a substantial but heterogeneous genetic component, and additional genetic factors remain to be identified.

The role of glycoprotein abnormalities in AD pathogenesis has been the focus of recent studies in this and other laboratories.[5-7] In normal core-1 glycosylation, *N*-acetylgalactosamine (GalNAc) is capped by galactose and sialic acid.[8,9] Transfer of galactose to GalNAc is mediated by C1GALT1/T-synthase enzyme, followed by the terminal addition of sialic acid.[10,11] The activity of T-synthase depends on the molecular chaperone C1GALT1C1/COSMC.[12] COSMC is required for folding, stability, and activity of T-synthase, and its disruption in mice results in

Tn antigen (CD175) expression and embryonic lethality.[13,14] Tn antigen was originally described in red cell polyagglutinability syndrome and subsequently in cancerous tissues and IgA nephropathy.[8,15,16] Tn antigen represents exposure of GalNAc, the basic molecule of mucin type glycoproteins, attached to serine, threonine, or tyrosine.[9,15] We previously observed an increase in Tn antigen expression in the cortices of AD patients.[7] This finding was supported by Frenkel et al., who demonstrated elevated Tn expression in the sera of AD subjects compared to normals, using vicia villosa lectin.[17]

In humans, among 100 known congenital disorders of glycosylation, about 30% reside in the *O*-glycosylation pathways.[18] Single nucleotide polymorphisms (SNPs) in genes account for several *O*-glycosylation disorders involving core-1 glycoproteins. In EOAD, an exome chip case-control association study and whole exome sequencing identified *T-synthase* as one of nine significant genes out of 7,249 genes tested.[19] In a microarray study on brain hippocampus from incipient AD cases, *T-synthase* was upregulated (http://www.ncbi.nlm.nih.gov/geo/query/acc.cgi?acc = GSE1297).[20] An in vitro study on human hippocampal progenitor cell lines over time evaluated the neurogenic impact of serum of individuals with mild cognitive impairment as they either progressed to AD (convertors) or remained stable (non-convertors), found COSMC to be one of the differentially expressed proteins [21]. Therefore, we investigated *COSMC* mutations and its effects on COSMC and T-synthase protein levels and T-synthase activity in LOAD and age-matched control (normal) brain tissues.

HIGHLIGHTS

- *C1GALT1C1/COSMC* mutations were found in late-onset Alzheimer's disease (AD) brains
- *C1GALT1C1/COSMC* coding mutations exhibit a positive correlation with AD progression
- *C1GALT1C1/COSMC* mutations do not affect COSMC protein levels

RESEARCH IN CONTEXT

1. Systematic review: During core-1 biosynthesis, GalNAc-linked to Ser/Thr, is capped by galactose forming Galβ3GalNAcα1-Ser/Thr (T-antigen), Transfer of galactose to GalNAc is catalyzed by C1GALT1/T-synthase that requires a molecular chaperone C1GALT1C1/COSMC. We tested Alzheimer's disease (AD) and age-matched normal brains tissues for *COSMC* mutations and their effects on COSMC and T-synthase protein levels, and on T-synthase activity.
2. Interpretation: Multiple *COSMC* mutations were detected in all groups. In advanced AD, *COSMC* coding mutations led to a significant reduction in T-synthase activity without significant effects on COSMC, although significantly elevating T-synthase protein levels suggesting reduced COSMC chaperone activity. Dysfunctions caused by *COSMC* mutations may initiate aberrant galactosylation in advanced AD.
3. Future directions: It is necessary to identify brain cells and regions in which *COSMC* mutations occur, to test larger number of samples, determine somatic or hereditary nature of the mutations, and establish their association and role in glycoproteome alterations and pathogenesis of AD.

2 | METHODS

2.1 | Human brain tissue

Frozen cortical samples from AD and age-matched normal brains were obtained from Kathleen Price Bryan Brain Bank of Duke University Medical Center, NC, USA, and from New South Wales (NSW) Tissue Resource Centre at the University of Sydney and the Sydney Brain Bank at Neuroscience Research Australia which are supported by the National Health and Medical Research Council of Australia, The University of New South Wales, Neuroscience Research Australia and Schizophrenia Research Institute. Research reported in this publication was supported by the National Institute On Alcohol Abuse And Alcoholism of the National Institutes of Health under Award Number R28AA012725. The content is solely the responsibility of the authors and does not necessarily represent the official views of the National Institutes of Health.

This study was approved by the institutional review board of Albert Einstein College of Medicine (AECOM), NY, USA vide number 2018-9204. The age, gender, postmortem delay, and Braak and Braak stages can be found in Supplementary Table 1. These include nine normal, five AD stage III (AD III), five AD stage V (AD V), and six AD stage VI (AD VI) samples. The AD V and AD VI were combined for analysis and have been labeled as AD VI-1 through AD VI-11 and collectively referred to as advanced AD. Control samples from age-matched donors without AD manifestation are referred as normals.

2.2 | Nucleic acid extractions

DNA and RNA from frozen brain tissues were extracted using DNeasy Blood and Tissue Kit (Qiagen, USA) and Trizol reagent (Invitrogen, USA) respectively. DNA and RNA concentrations were measured using a nanodrop ND-1000 spectrophotometer (Thermo Scientific, USA).

2.3 | Polymerase chain reaction and Sanger sequencing

Polymerase chain reaction (PCR) was carried out in 25 µL volume using 500 ng DNA, AmpliTaq Gold 360 master mix (Applied Biosystems Inc.,

USA), *C1GALT1C1* gene specific primers for the two exons (RefSeq NM_001011551) in a MJ Research PTC-200 Thermal Cycler (Biorad Laboratories Inc., USA) at 59°C annealing temperature. The forward and reverse primers for exon 1 were pF1: 5′ACGCAGGCCTATAGCAAGTC3′ and pR1: 5′TCCTGTGCTGACAATCCTCC3′. Exon 2 was amplified using two overlapping primer pairs to span the entire length. The two forward primers were pF2a: 5′TGATTTCAAGCTTGGGAACCTTT3′ and pF2b: 5′TTGAAAATATGCCCAAATGCCCT3′, and the two reverse primers were pR2a: 5′TGAGAAAAGCTTACAAATACGCCT3′, and pR2b: 5′CATTGGAACTTGGGGAGGCT3′. The PCR products were analyzed on a 1% agarose gel in Tris-acetate-EDTA buffer. The PCR products were purified with QIAquick PCR purification kit (Qiagen Inc., USA) and subjected to Sanger sequencing at the Genomics Core Facility at AECOM supported by the Cancer Center Support Grant (P30 CA013330).

2.4 | Real Time Quantitative RT-PCR

Real-Time Quantitative Reverse Transcription PCR (Q-RT-PCR) for *COSMC* and *T-synthase* was performed at the Genomics Core Facility at AECOM. cDNA was prepared from 500 ng of total RNA using superscript vilo master mix (Invitrogen, USA). Real time Q-RT-PCR was performed using Taqman fast advanced master mix and primer probe mix (Life Technologies, USA) in an 8 µL reaction volume in 7900 HT Fast Real time PCR system (Applied Biosystems, USA) with Taqman assays (Supplementary Table 2) as per manufacturer's instructions. The housekeeping gene used was 18S ribosomal RNA. The TaqMan minor groove binder probes with 6-carboxyfluorescein (FAM) as 5′ fluorophore and a 3′ non-fluorescent quencher were used. The padded amplicon sequences detected by the Taqman assays are provided in Table S3. Fold changes were calculated using the $2^{-\Delta\Delta Ct}$ method and plotted as fold differences of relative gene expression normalized to controls.

2.5 | Western blotting

Brain homogenates were prepared by sonication using 1 g of cortex in 10 mL of lysis buffer [tris buffered saline, pH 7.4 with sodium fluoride, sodium orthovanadate, EGTA, Triton–X-100] containing complete mini protease inhibitor cocktail (Roche, USA). Supernatants were prepared by centrifugation of homogenates for 10 minutes at 4°C at 14,000 RPM in an Eppendorf 5418R centrifuge. Protein concentrations were measured using the Bradford assay (Biorad Laboratories, USA).[21] Supernatants were heated at 55°C, whereas homogenates were heated at 95°C for 5 minutes prior to loading on a gel. Twenty micrograms protein was subjected to electrophoresis on NuPAGE 10% Bis-Tris protein gels and transferred to PVDF membranes (EMD Millipore, USA) using NuPAGE gel electrophoresis system (Invitrogen, USA). Membranes were blocked with 5% non-fat dry milk (Omnipur, Calbiochem, USA) in TBST (0.05% Tween 20) and incubated overnight at 4°C with primary antibodies. Brain homogenates were probed with rabbit anti-beta Amyloid D54D2 (Cell Signaling 1:2000), while supernatants were probed with mouse anti-COSMC H-10 (Santa Cruz 1-1000) and rabbit anti-C1GALT1: PA5-43363 (Invitrogen 1-1000). Secondary antibodies used were HRP anti-rabbit (Invitrogen 1:10000) or HRP anti-mouse (Millipore 1:2000). The results were visualized with chemiluminescence reagent (Kindle Bioscience; USA) and quantified by analyzing densitometry with ImageJ. Normalization was performed with anti-actin [mouse anti-actin (Calbiochem 1:7000) for COSMC and amyloid β [Aβ]; HRP anti-mouse mu chain specific (Invitrogen 1:10000) and rabbit anti-human actin (Invitrogen 1:1000) for T-synthase; HRP goat anti rabbit IgG (H+L) Abcam GR 3192715-6]. The mouse anti-actin antibody cross reacts with human actin as well as actin from several species.

2.6 | T-synthase activity assay

T-synthase activity was measured in supernatants from AD and normal brain tissue using a fluorescent assay developed by Ju and Cummings.[22,23] Reagents for the assay included UDP-Gal as donor (Millipore Sigma, USA), GalNAc-α-(4-methylumbelliferone) (GalNAc-α-(4-MU)) as acceptor (Carbosynth Limited, UK), and 7-Hydroxy-4-MU (Alfa Aesar, USA). The reaction product was cleaved by endo-α-*N*-acetylgalactosaminidase (New England Biolabs, USA) to release 4-methylumbelliferone (4-MU), which is fluorescent. To generate a standard curve, 4-MU was dissolved in DMSO to make a 1 mM stock solution, followed by dilutions in 0.5 mM MES-NaOH buffer (pH 6.8) to achieve a range of concentrations between 10 and 20,000 nM; 50 µL of each concentration was loaded in triplicate into a 96 well black plate (Corning, USA) and incubated on a rocker at 37°C for 2 hours prior to adding 100 µL of stop solution (1 M Glycine-NaOH, pH 10.0). The fluorescence was measured using a spectrophotometer (Molecular Devices, USA) at excitation and emission wavelengths of 355 and 460 nm, respectively.

For the assay, 10 µL supernatant was mixed with 1000 µM GalNAc-α-(4-MU), 500 µM UDP-Gal, 20 mM $MnCl_2$, and 800 units of *O*-Glycosidase in 50 mM MES-NaOH buffer (pH 6.8) and incubated at 37°C for 2 hours on a rocker. Subsequently, 100 µL of stop solution was added and the fluorescence units were measured. In blank reactions deionized water replaced UDP-Gal.[23] T-synthase activity was calculated as pmol/h-mg protein by dividing T-synthase activity (pmol/hr-ml) by the protein concentration (mg/mL) determined by Biorad assays.

2.7 | Statistical analysis

Statistical analysis was performed using SigmaStat (Systat Software). Analysis of variance (ANOVA) between the groups was performed. All P values ≤ 0.05 were statistically significant and denoted by *, whereas P values ≤ 0.01 were denoted by **.

TABLE 1 *COSMC* mutations in promoter, coding region and 3′UTR in Alzheimer's disease and age-matched normal brain samples.

Case number	Promoter	Coding region	3′UTR
Normal 1	None	g.4376T>A, p.D131E¶	c.*237T>G
Normal 2	g.-3044G>T + g.-3043G>T and g.-3018G>A	None	c.*237T>G
Normal 3	g.-3044G>T + g.-3043G>T	None	None
Normal 4	g.-3044G>T + g.-3043G>T and g.-3018G>A	None	None
Normal 5	g.-3044G>T + g.-3043G>T and g.-3018G>A	None	None
Normal 6	g.-3044G>T + g.-3043G>T	g.4376T>A, p.D131E¶ + g. 4411C>T, p.A143V¶ + homozygous g.4656_4657 insT, p.C226X¶¶	c.*132_133InsA + c.*237_238InsT + c.241_242InsA
Normal 7	g.-3044G>T + g.-3043G>T	None	c.*23G>A + c.*87G>A
Normal 8	g.-3044G>T + g.-3043G>T and homozygous g.-3018G>A	g.4589A>C; p.N202T¶¶	None
Normal 9	g.-3044G>T + g.-3043G>T and g.-3018G>A	None	c.*235_236InsG
AD III-1	g.-3044G>T + g.-3043G>T	None	None
AD III-2	None	None	None
AD III-3	None	g.4616_4617InsA +g.4643_4644 InsA, p.G212RfsX219¶¶	None
AD III-4	None	None	None
AD III-5	g.-3044G>T + g.-3043G>T and g.-3018G>A	g.4936A>T, p.D318V¶¶	None
AD VI-1	g.-3044G>T + g.-3043G>T	g.4376T>A, p.D131E¶	None
AD VI-2	g.-3044G>T + g.-3043G>T and g.-3018G>A	None	c.*22T>G + c.*87G>A
AD VI-3	g.-3044G>T + g.-3043G>T	None	None
AD VI-4	g.-3018G>A	None	None
AD VI-5	None	g.4376 T>A, p.D131E¶	None
AD VI-6	g.-3044G>T + g.-3043G>T	g.4376T>A, p.D131E¶ + g.*1 G >T¶¶	c.*178T> C + c.*215A>C
AD VI-7	g.-3044G>T + g.-3043G>T	g.4376T>A, p.D131E¶	None
AD VI-8	g.-3044G>T + g.-3043G>T	None	c.*107_108InsA + c.*214_215InsA
AD VI-9	g.-3044G>T + g.-3043G>T and g.-3018G>A	g.4588A>C, p.N202T¶¶	c.*137_138InsA + c.*177_178InsT
AD VI-10	g.-3044G>T + g.-3043G>T and g.-3018G>A	None	None
AD VI-11	g.-3044G>T + g.-3043G>T	Homozygous g.4376T>A, p.D131E¶	c.*218_219InsT

¶¶Are unique mutations and ¶ are mutations found in gnomAD database.

3 | RESULTS

3.1 | *COSMC* mutations in brain tissues

PCR of *COSMC* to amplify exon 1 and exon 2 from normal and AD brain tissues revealed that all groups had mutations in *COSMC* in varying percentages in promotor, coding region, as well as 3′UTR. No mutations were found in 5′UTR or exon 1 (Table 1).

3.1.1 | Promoter mutations

Substitution mutations at three unique locations in the *COSMC* promoter were found in common across AD and normal brain samples (Figure S1). Co-occurrence of three promoter mutations (g.-3044G>T, g.-3043G>T, and g.-3018G>A) was exhibited at a higher percentage in normal brain samples (56%) as compared to AD VI (27%). This is inverse to the co-occurrence of double promoter mutations (g.-3044G>T and

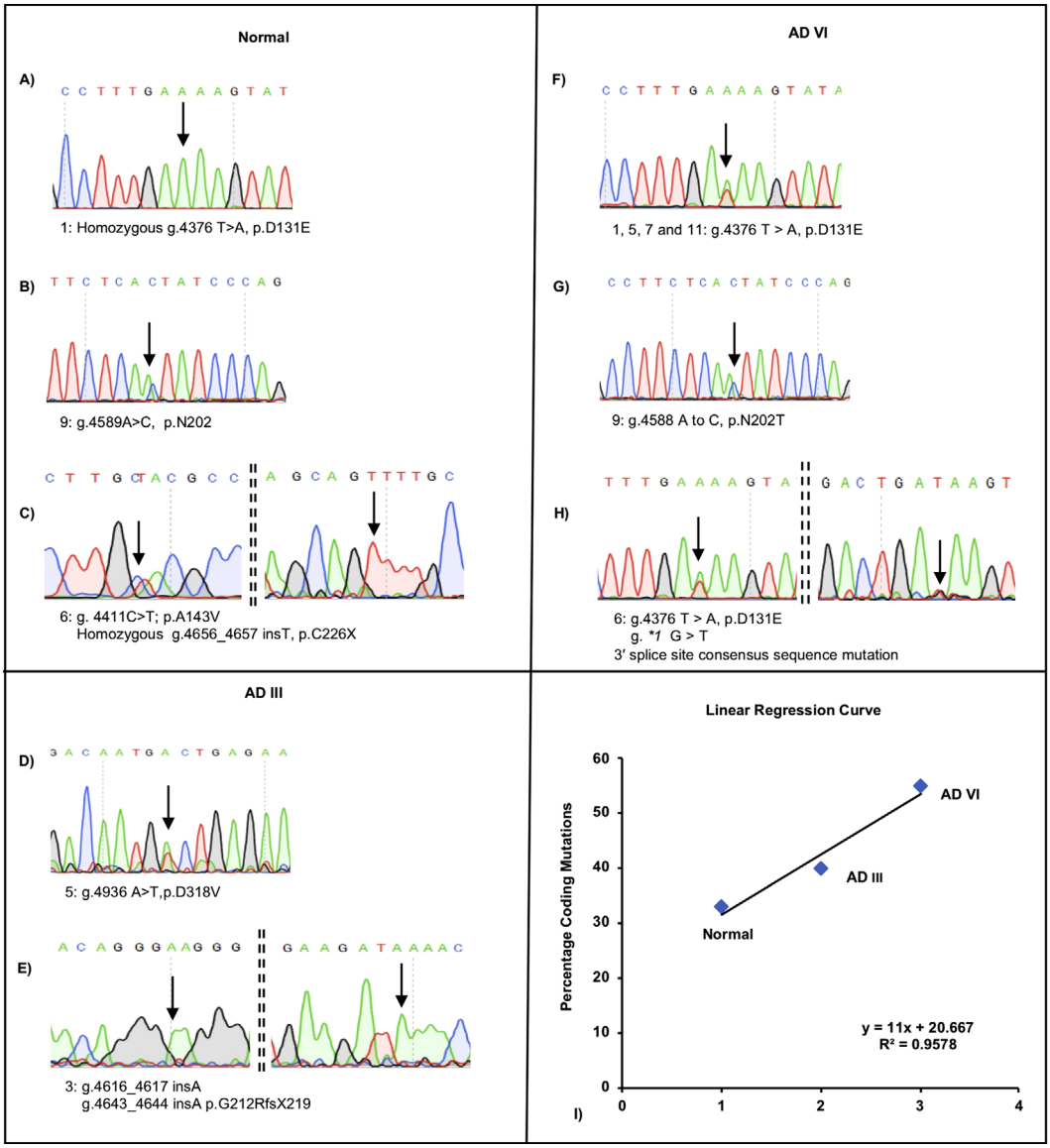

FIGURE 1 *COSMC* coding mutations in normals, AD III, and AD VI. (A) Normal-1, (B) Normal-9, (C) Normal-6, (D) AD III-5, (E) AD III-3, (F) AD VI-1, AD VI-5, AD VI-7, and AD VI-11, (G) AD VI-9, (H) AD VI-6, and (I) A linear regression curve for percentage of coding mutations with disease severity.

g.-3043G>T), which is lower in normal (33%) and higher in AD VI (55%). Sample AD VI-4 had only a single g.-3018G>A substitution, which was previously identified as SNP rs3810744 (https://www.ncbi.nlm.nih.gov/snp/rs3810744). The *COSMC* coding variations common to those previously described in the Genome Aggregation Database (https://gnomad.broadinstitute.org/gene/ENSG00000171155) are denoted by † while the unique coding variations are denoted by †† (Table 1).

3.1.2 | Coding mutations

The mutations observed in normal, AD III, and AD VI are depicted in Figure 1A-H. A linear regression curve indicated that the percentage of coding mutations positively correlates with the progression of the disease (Rš = 0.9578) (Figure 1I). The most frequently observed mutation in the coding region of *COSMC* was g.4376T > A, p.D131E, found in 45.5% of all AD VI and 22.2% of normals. Sample AD VI-6 also has a 3′ consensus splice site mutation (g.*1G>T) (Figure 1H). A single frameshift mutation in Sample AD III-3 due to two independent insertion events resulted in p.G212RfsX219 (Figure 1E).

3.1.3 | 3′UTR mutations

The percentage of 3′UTR mutations in normal and AD VI were 56% and 45% (Figure S2). None of the AD III samples had 3′UTR mutations.

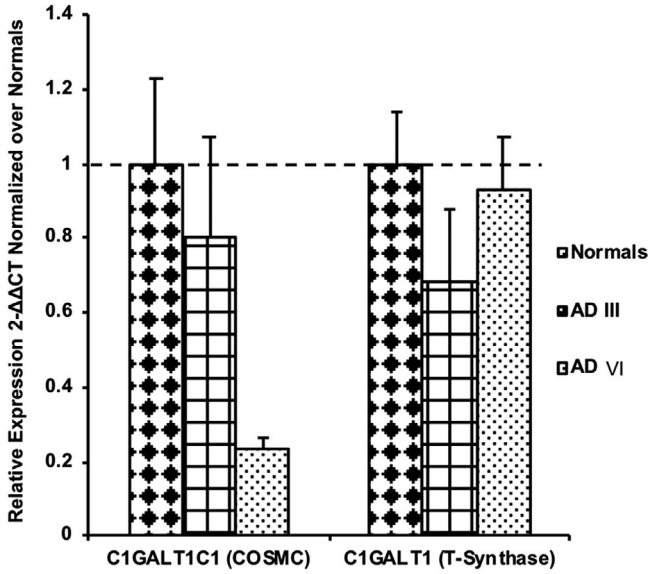

FIGURE 2 Real time quantitative RT-PCR for *C1GALT1/T-synthase* and *CIGALT1C1/COSMC* in normals, AD III, and AD VI

60% of AD samples had double variations in 3′UTR, which included double substitutions or double insertion events (Figure S2E-I). The AD VI samples that expressed 3′UTR variations were surprisingly homozygous in AD VI (Figure S2F-I) except for AD VI-2, which was heterozygous (Figure S2E). The normal brains also had 3′UTR mutations (Figure S2A-D). Normal-6 had homozygous insertions (Figure S2A) unlike the rest of the normals with heterozygous variations (Figure S2B-D).

In summary, the frequency of *COSMC* mutations in the prefrontal cortex of AD brains was almost twice that of normal brains. A linear regression curve indicated that the number of mutations increased with AD progression.

3.2 | Q-RT-PCR of *T-synthase* and *COSMC*

Taqman assays were performed to investigate differences in RNA expression of *COSMC* and *T-synthase* in AD and normal brains using 18S as housekeeping gene. *COSMC* RNA expression demonstrated a trend: AD VI < AD III < Normals (Figure 2). AD VI and AD III had 4.2-fold and 1.2-fold lower *COSMC* expression, respectively, as compared to normals. The expression of *T-synthase* between the groups did not demonstrate a trend. The expression levels between the groups were not significantly different for either *COSMC* or *T-synthase*. In summary, *COSMC* mutations did not significantly reduce expression of *COSMC* or *T-synthase* RNA expression.

3.3 | Western blot

Western blot analysis was performed using antibodies against COSMC, T-synthase, and Aβ antibodies to examine the effects of COSMC coding mutations on these proteins. There were no significant differences in COSMC protein expression between the normal, AD III, or AD VI brains with and without mutations (Figure 3A and B).

T-synthase antibody revealed protein monomers at 52 kDa and dimers at 102 kDa (Figure 3C). ImageJ analysis of pooled bands revealed significantly higher T-synthase levels in advanced AD with mutations as compared to normals with mutations ($P = 0.03$) and normals without mutations ($P = 0.01$) (Figure 3D). Analyzing the dimer band independently in samples with mutations, advanced AD had higher levels compared to normals ($P = 0.034$). In addition, in samples without mutations, advanced AD exhibited higher T-synthase levels compared to normals and AD III (Figure 3D). In all samples without factoring *COSMC* coding mutations, advanced AD again exhibited significantly higher T-synthase levels compared to normals ($P = 0.0028$) and AD III ($P = 0.032$) (Figure 3E).

The Aβ antibody was used to investigate a possible relationship with COSMC (Figure 4A). The 4 kDa Aβ band was significant in AD III ($P = 0.001$) and AD VI ($P = 0.046$) when compared to normals without *COSMC* coding mutations (Figure 4B). The high-molecular-weight Aβ multimers were also present in all AD samples (Figure 4A). Three normal samples with mutations classified as normal and without significant neuropathology, displayed a 4 kDa Aβ band at levels comparable to AD brain samples and significantly higher than normals without mutations ($P = 0.047$) (Figure 4A). In addition, these samples also had the same mutations as observed in AD VI. In conclusion, *COSMC* coding mutations did not significantly influence COSMC but resulted in an elevation of T-synthase protein in advanced AD.

3.4 | T-synthase activity assay

T-synthase activity was measured in supernatants to determine the effects of *COSMC* mutations on T-synthase (Figure 5). No significant differences in T-synthase activity were observed when results were compared without factoring coding mutations. Separating the groups based on presence or absence of *COSMC* coding mutations revealed a significant difference. The AD VI without *COSMC* coding mutations had 3.1-fold higher T-synthase activity when compared to AD VI with coding mutations ($P = 0.01$). In addition, in the presence of coding mutations, AD VI had significantly lower T-synthase activity as compared to both AD III ($P = 0.03$) and normal brain ($P = 0.001$). T-synthase activity in AD VI with *COSMC* coding mutations were significantly lower as compared to AD III and normal with mutations as well as AD VI without *COSMC* coding mutations.

4 | DISCUSSION

Based on previous findings that glycoprotein abnormalities may play a role in LOAD pathogenesis, this study focused on *COSMC* gene mutations and T-synthase activity, the essential factors in biosynthesis and integrity of mucin type glycoproteins. Common genetic variations in these genes can influence *O*-glycosylation.[24,25] This is the first report

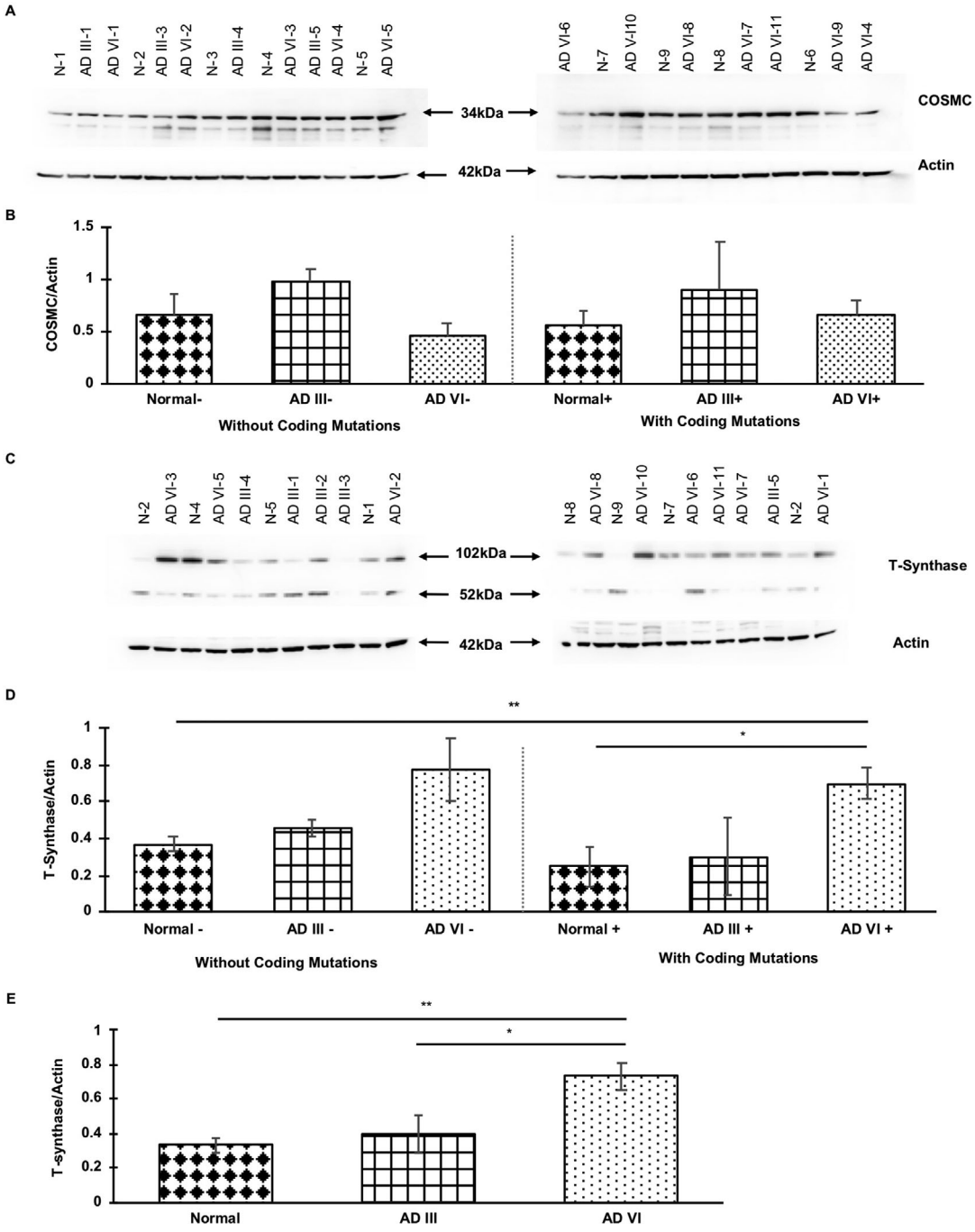

FIGURE 3 Western blot and ImageJ analysis in normal, AD III, and AD VI brain samples with and without *COSMC* coding mutations. (A) Western analysis with COSMC and actin antibodies. (B) ImageJ analysis of COSMC western blot. (C) Western analysis with T-synthase and actin antibodies and (D) ImageJ analysis of T-synthase western blot. + are with *COSMC* coding mutation and - are without *COSMC* coding mutation. * represents significance at $P \leq 0.05$ and ** represents significance at $P \leq 0.01$. (E) ImageJ analysis of T-synthase western blot irrespective of *COSMC* coding mutations. * represents significance at $P \leq 0.05$ and ** represents significance at $P \leq 0.01$

on *COSMC* mutations in the coding region, promoter region, and 3′UTR in both AD and normal brains.

In the coding region, the p.D131E was the most common mutation observed in 22.2% of normals and 45.45% of advanced AD subjects. This SNP, formerly known as c.628T > A [ncbi: s17261572], was reported in 32% of 120 healthy Europeans.[26] A functional role of this SNP had not yet been established with any human diseases. T-synthase protein levels in advanced AD were higher than normals and AD III, probably due to the failure of clearance of aggregated and misfolded proteins.[26] In the absence of COSMC in cultured cells, T-synthase protein cannot fold to become active and aggregates.[27] The binding of COSMC to sequester T-synthase to promote its folding may prevent

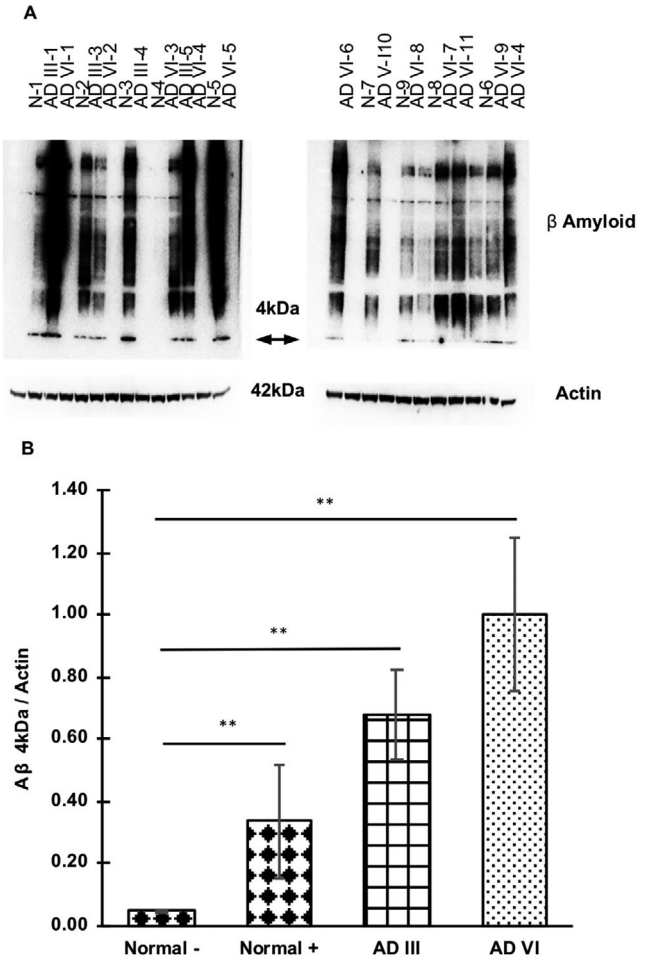

FIGURE 4 (A) Western analysis with Aβ and actin antibodies. (B) ImageJ analysis of Aβ western blot. Normal + are with *COSMC* coding mutation while Normal – are without *COSMC* coding mutations. * represents significance at $P \leq 0.05$ and ** represents significance at $P \leq 0.01$

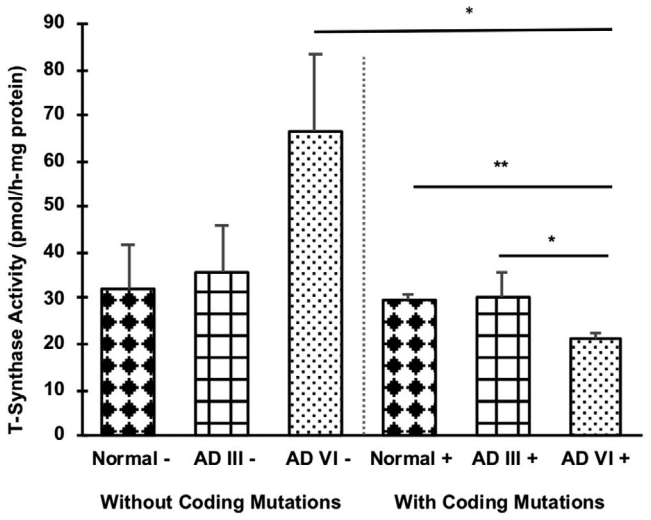

FIGURE 5 (A) T-synthase activity assay of brain supernatants in normals, AD III, and AD VI with and without *COSMC* coding mutations. + are with *COSMC* coding mutation and - are without *COSMC* coding mutations. * represents significance at $P \leq 0.05$ and ** represents significance at $P \leq 0.01$

T-synthase from forming oligomers. We observed T-synthase monomers and dimers and low T-synthase activity indicative of dysfunctional COSMC and the likely inability of COSMC to sequester T-synthase protein.

Our observations indicate that *COSMC* coding mutations influence T-synthase activity without altering COSMC protein levels. The supernatants prepared from the brain tissues without coding mutations exhibited 3.1-fold higher T-synthase activity compared to advanced AD brains with coding mutations. Comparing the coding mutation positive cases, advanced AD had significantly lower T-synthase activity compared to AD III and normals despite significantly higher T-synthase protein. This supports the conclusion that reduced T-synthase activity in AD with *COSMC* coding mutations is due to failure of COSMC activation of T-synthase. The effects of *COSMC* mutations on T-synthase activity in normals and advanced AD are different. We presume that these differences are related to the pathological changes in AD brain: the mutant COSMC protein can activate T-synthase in a normal brain environment but cannot function in the pathological environment in the advanced AD. This effect of the environment may also explain why no effects had been previously recognized for p.D131E mutation, which was tested only in normals.[26]

COSMC mutations resulting in Tn antigen expression have been shown to cause several diseases.[16,28] However, in vivo and in vitro effects of *COSMC* mutations may differ. Two COSMC mutant proteins p.Δ256 and p.E152K are functional in vitro; however, p.E152K shows loss of function and increased Tn antigen expression in vivo.[28,29] COSMC p.E152K mutation, originally identified in polyagglutinability syndrome, was not observed in our study. Loss of functional COSMC by mutation, deletion, or hypermethylation may contribute to Tn expression. For a better understanding of the role of *COSMC* mutations in the pathophysiology of LOAD functional studies are necessary considering the complex interplay between genes and environment in aging brains.

Aging has been shown to increase somatic mutation, which may be responsible for late-onset neurodegenerative diseases like AD.[30,31] In our cohort, the average age of the Duke AD samples was 17 years younger than that of NSW AD samples, whereas the average age of the Duke normal brains was 10 years younger than that of NSW normal brains. These age differences may account for the higher mutation incidence observed in the NSW samples. Given that the COSMC protein levels did not differ between the groups with and without mutations, it suggests that brain *COSMC* mutations have a somatic origin.

COSMC is located on the X-chromosome and in this study several female subjects had homozygous variations (Table 1). Two of the NSW females, normal-6 and normal-8 (ages 102 and 97), had the same *COSMC* coding mutations as advanced AD cases and significantly higher amounts of Aβ (Figure 4). The pathological determination of AD, however, is not solely dependent upon amyloid accumulation. As seen in many studies, age-matched individuals who are

cognitively normal have high amyloid deposits comparable to AD subjects.[32] The updated National Institute on Aging and the Alzheimer's Association's neuropathological guidelines acknowledge the potential disconnect between the clinical picture and neuropathological changes.[32-34]

Similar to the coding region, SNPs and modifications in the promoter region can cause changes in the expression of COSMC.[35,36] In our study, three SNPs g.-3044G>T, g.-3043G>T, and g.-3018G>A were observed in *COSMC* promoter. SNP g.-3018G>A (rs3810744) has been reported in IgA nephropathy, a disorder that also expresses Tn antigen.[37] Future studies should explore the relevance of *COSMC* promoter mutations in AD. Both *COSMC* and T-synthase are under the control of Krüppel-like transcription factors (TFs), the expression of which varies substantially in different tissues.[36] The Krüppel-like factors (KLFs), including SP1/SP3 are a family of ubiquitously expressed proteins that regulate target gene transcription.[36] Basal levels of human COSMC and T-synthase are transcriptionally regulated by KLF SP1/3 TFs and regulate other cell- or tissue-specific TFs. Several glycosyltransferases involved in *O*-glycan biosynthesis are also under the control of SP1. Reporting for the first time, the unique *COSMC* promoter mutations at g.-3043 and g.-3044 fall in the KLF region and probably contribute to the variable expression of COSMC and T-synthase, which needs further investigation.

COSMC 3′UTR has binding sites for multiple micro RNAs (miRNAs) such as hsa-miR-448 as predicted by www.targetscan.org. The miRNAs bind to 3′UTR and regulate gene expression mediated by miRNA response elements (MREs). SNPs in 3′UTR contribute to disease pathogenesis including AD.[38,39] In LOAD, 35 miRNAs in the hippocampus and 41 miRNAs in the prefrontal cortex are deregulated.[40] In LOAD, three MRE-SNPs in 3′UTRs of the genes; TF CP2, granulin, and insulin degrading enzyme alter their binding to miRNAs.[41] In another study, miR-374 levels were significantly diminished in AD, which may target the AD gene beta-secretase 1 (*BACE1*).[42] However, the significance of our 3′UTR mutations in mi-RNA binding in LOAD and glycoproteome needs further analysis.

Brains of AD patients display an altered profile of protein *O*-glycosylation, sialylation, and *N*-glycosylation.[43,44] Both *O*-GlcNAcylation and *O*-GalNAcylation have been found to play a role in AD.[45,46] Many of the AD-related proteins, including APP, TAU, BACE1, nicastrin, are functionally modified by glycosylation in AD pathogenesis.[43,47-49] The interplay between Tn antigen, T antigen, COSMC, T-synthase, and sialylation needs further exploration in AD. Taken together, our results demonstrate that in advanced AD the *COSMC* coding mutations cause a significant reduction of T-synthase activity. The effects may be mediated through reduced galactosylation. There exists a need for evaluation of a larger number of AD patients for mutations in *COSMC* to establish an association with AD.

ACKNOWLEDGMENTS

This project was supported by Mr. Jeffrey and Mrs. Marieke Rothschild.

DECLARATIONS OF INTEREST

The authors declare no conflict of interest.

REFERENCES

1. Cruchaga C, Del-Aguila JL, Saef B, et al. Polygenic risk score of sporadic late-onset Alzheimer's disease reveals a shared architecture with the familial and early-onset forms. *Alzheimers Dement*. 2018;14(2):205-214.
2. Giau VV, Senanarong V, Bagyinszky E, An SSA, Kim S. Analysis of 50 neurodegenerative genes in clinically diagnosed early-onset Alzheimer's disease. *Int J Mol Sci*. 2019;20(6):1514.
3. Corder EH, Saunders AM, Strittmatter WJ, et al. Gene dose of apolipoprotein E type 4 allele and the risk of Alzheimer's disease in late onset families. *Science*. 1993;261(5123):921-923.
4. Durmaz A, Kumral E, Durmaz B, et al. Genetic factors associated with the predisposition to late onset Alzheimer's disease. *Gene*. 2019;707:212-215.
5. Schedin-Weiss S, Winblad B, Tjernberg LO. The role of protein glycosylation in Alzheimer disease. *FEBS J*. 2014;281(1):46-62.
6. Regan P, McClean PL, Smyth T, Doherty M. Early stage glycosylation biomarkers in Alzheimer's disease. *Medicines*. 2019;6(3):92.
7. Lalezari P, Lekhraj R, Kimiabakhsh B, Carrasco E, Casper D. Tn antigen in the brain: a newly recognized glycoprotein in Alzheimer's disease. *Alzheimer's & Dementia*. 2013;9(4, Supplement):P347-P348.
8. Ju T, Cummings RD. Protein glycosylation: chaperone mutation in Tn syndrome. *Nature*. 2005;437(7063):1252.
9. Ju T, Otto VI, Cummings RD. The Tn antigen-structural simplicity and biological complexity. *Angew Chem Int Ed Engl*. 2011;50(8):1770-1791.
10. Wells L, Feizi T. Editorial overview: carbohydrates: O-glycosylation. *Curr Opin Struct Biol*. 2019;56:iii-v.
11. de las Rivas M, Lira-Navarrete E, Gerken TA, Hurtado-Guerrero R. Polypeptide GalNAc-Ts: from redundancy to specificity. *Curr Opin Struct Biol*. 2019;56:87-96.
12. Aryal RP, Ju T, Cummings RD. Tight complex formation between Cosmc chaperone and its specific client non-native T-synthase leads to enzyme activity and client-driven dissociation. *J Biol Chem*. 2012;287(19):15317-15329.
13. Wang Y, Ju T, Ding X, et al. Cosmc is an essential chaperone for correct protein O-glycosylation. *Proc Natl Acad Sci U S A*. 2010;107(20):9228-9233.
14. Crew VK, Singleton BK, Green C, Parsons SF, Daniels G, Anstee DJ. New mutations in C1GALT1C1 in individuals with Tn positive phenotype. *Br J Haematol*. 2008;142(4):657-667.
15. Berger EG. Tn-syndrome. *Biochim Biophys Acta*. 1999;1455(2):255-268.
16. Ju T, Wang Y, Aryal RP, et al. Tn and sialyl-Tn antigens, aberrant O-glycomics as human disease markers. *Proteomics Clin Appl*. 2013;7(9-10):618-631.
17. Frenkel-Pinter M, Shmueli MD, Raz C, et al. Interplay between protein glycosylation pathways in Alzheimer's disease. *Sci Adv*. 2017;3(9):e1601576.
18. van Tol W, Wessels H, Lefeber DJ. O-glycosylation disorders pave the road for understanding the complex human O-glycosylation machinery. *Curr Opin Struct Biol*. 2019;56:107-118.
19. Pericak-Vance M. *Whole Exome Analysis of Early Onset Alzheimer's Disease*. University of Miami: Miami, United States; 2018. https://apps.dtic.mil/dtic/tr/fulltext/u2/1064060.pdf.
20. Blalock EM, Geddes JW, Chen KC, Porter NM, Markesbery WR, Landfield PW. Incipient Alzheimer's disease: microarray correlation analyses reveal major transcriptional and tumor suppressor responses. *Proc Natl Acad Sci U S A*. 2004;101(7):2173-2178.
21. Maruszak A, Murphy T, Liu B, De Lucia C, Douiri A, Nevado AJ, Teunissen CE, Visser PJ, Price J, Lovestone S, Thuret S. Cellular phenotyping of hippocampal progenitors exposed to patient serum predicts progression to Alzheimer's Disease. *SSRN Electronic Journal*, http://doi.org/10.2139/ssrn.3459560.

22. Livak KJ, Schmittgen TD. Analysis of relative gene expression data using real-time quantitative PCR and the 2(-Delta Delta C(T)) Method. *Methods*. 2001;25(4):402-408.
23. Ju T, Cummings RD. A fluorescence-based assay for Core 1 beta3galactosyltransferase (T-synthase) activity. *Methods Mol Biol*. 2013;1022:15-28.
24. Ju T, Xia B, Aryal RP, et al. A novel fluorescent assay for T-synthase activity. *Glycobiology*. 2011;21(3):352-362.
25. Kiryluk K, Li Y, Moldoveanu Z, et al. GWAS for serum galactose-deficient IgA1 implicates critical genes of the O-glycosylation pathway. *PLoS Genet*. 2017;13(2):e1006609.
26. Gale DP, Molyneux K, Wimbury D, et al. Galactosylation of IgA1 is associated with common variation in C1GALT1. *J Am Soc Nephrol*. 2017;28(7):2158-2166.
27. Malycha F, Eggermann T, Hristov M, et al. No evidence for a role of cosmc-chaperone mutations in European IgA nephropathy patients. *Nephrol Dial Transplant*. 2009;24(1):321-324.
28. Aryal RP, Ju T, Cummings RD. Identification of a novel protein binding motif within the T-synthase for the molecular chaperone Cosmc. *J Biol Chem*. 2014;289(17):11630-11641.
29. Sun X, Ju T, Cummings RD. Differential expression of Cosmc, T-synthase and mucins in Tn-positive colorectal cancers. *BMC Cancer*. 2018;18(1):827.
30. Hanes MS, Moremen KW, Cummings RD. Biochemical characterization of functional domains of the chaperone Cosmc. *PLoS One*. 2017;12(6):e0180242.
31. Park JS, Lee J, Jung ES, et al. Brain somatic mutations observed in Alzheimer's disease associated with aging and dysregulation of tau phosphorylation. *Nat Commun*. 2019;10(1):3090.
32. Lodato MA, Walsh CA. Genome aging: somatic mutation in the brain links age-related decline with disease and nominates pathogenic mechanisms. *Hum Mol Genet*. 2019;28(R2):R197-R206.
33. Lane CA, Hardy J, Schott JM. Alzheimer's disease. *Eur J Neurol*. 2018;25(1):59-70.
34. Hyman BT, Phelps CH, Beach TG, et al. National Institute on Aging-Alzheimer's Association guidelines for the neuropathologic assessment of Alzheimer's disease. *Alzheimers Dement*. 2012;8(1):1-13.
35. Mecocci P, Baroni M, Senin U, Boccardi V. Brain aging and late-onset Alzheimer's disease: a matter of increased amyloid or reduced energy. *J Alzheimers Dis*. 2018;64(s1):S397-S404.
36. Liu Y, Wang M, Marcora EM, Zhang B, Goate AM. Promoter DNA hypermethylation—Implications for Alzheimer's disease. *Neurosci Lett*. 2019;711:134403.
37. Zeng J, Mi R, Wang Y, et al. Promoters of human Cosmc and T-synthase genes are similar in structure, yet different in epigenetic regulation. *J Biol Chem*. 2015;290(31):19018-19033.
38. Li GS, Nie GJ, Zhang H, Lv JC, Shen Y, Wang HY. Do the mutations of C1GALT1C1 gene play important roles in the genetic susceptibility to Chinese IgA nephropathy. *BMC Med Genet*. 2009;10:101.
39. Le MT, Xie H, Zhou B, et al. MicroRNA-125b promotes neuronal differentiation in human cells by repressing multiple targets. *Mol Cell Biol*. 2009;29(19):5290-5305.
40. Juzwik CA, S SD, Zhang Y, et al. microRNA dysregulation in neurodegenerative diseases: a systematic review. *Prog Neurobiol*. 2019;182:101664.
41. Lau P, Bossers K, Janky R, et al. Alteration of the microRNA network during the progression of Alzheimer's disease. *EMBO Mol Med*. 2013;5(10):1613-1634.
42. Roy J, Mallick B. Altered gene expression in late-onset Alzheimer's disease due to SNPs within 3′UTR microRNA response elements. *Genomics*. 2017;109(3):177-185.
43. Manzine PR, Pelucchi S, Horst MA, et al. microRNA 221 targets ADAM10 mRNA and is downregulated in Alzheimer's disease. *J Alzheimers Dis*. 2018;61(1):113-123.
44. Kanninen K, Goldsteins G, Auriola S, Alafuzoff I, Koistinaho J. Glycosylation changes in Alzheimer's disease as revealed by a proteomic approach. *Neurosci Lett*. 2004;367(2):235-240.
45. Butterfield DA, Owen JB. Lectin-affinity chromatography brain glycoproteomics and Alzheimer disease: insights into protein alterations consistent with the pathology and progression of this dementing disorder. *Proteomics Clin Appl*. 2011;5(1-2):50-56.
46. Wani WY, Chatham JC, Darley-Usmar V, McMahon LL, Zhang J. O-GlcNAcylation and neurodegeneration. *Brain Res Bull*. 2017;133:80-87.
47. Akasaka-Manya K, Kawamura M, Tsumoto H, et al. Excess APP O-glycosylation by GalNAc-T6 decreases Aβ production. *J Biochem*. 2016;161(1):99-111.
48. Kizuka Y, Kitazume S, Fujinawa R, et al. An aberrant sugar modification of BACE1 blocks its lysosomal targeting in Alzheimer's disease. *EMBO Mol Med*. 2015;7(2):175-189.
49. Lassen PS, Thygesen C, Larsen MR, Kempf SJ. Understanding Alzheimer's disease by global quantification of protein phosphorylation and sialylated N-linked glycosylation profiles: a chance for new biomarkers in neuroproteomics. *J Proteomics*. 2017;161:11-25.
50. Taniguchi N, Takahashi M, Kizuka Y, et al. Glycation vs. glycosylation: a tale of two different chemistries and biology in Alzheimer's disease. *Glycoconj J*. 2016;33(4):487-497.

SUPPORTING INFORMATION

Additional supporting information may be found online in the Supporting Information section at the end of the article.

How to cite this article: Gollamudi S, Lekhraj R, Lalezari S, Lalezari P. *COSMC* mutations reduce T-synthase activity in advanced Alzheimer's disease. *Alzheimer's Dement*. 2020;6:e12040. https://doi.org/10.1002/trc2.12040